

## Biofilm Development and Destruction in Turbulent Flow

W.G. Characklis

To cite this article: W.G. Characklis (1979) Biofilm Development and Destruction in Turbulent Flow, Ozone: Science & Engineering, 1:2, 167-181, DOI: [10.1080/01919517908550842](https://doi.org/10.1080/01919517908550842)

To link to this article: <http://dx.doi.org/10.1080/01919517908550842>



Published online: 23 Jul 2008.



Submit your article to this journal [↗](#)



Article views: 30



View related articles [↗](#)



Citing articles: 1 View citing articles [↗](#)

BIOFILM DEVELOPMENT AND DESTRUCTION  
IN TURBULENT FLOW

W.G. Characklis

Rice University  
Department of Environmental Science and Engineering  
Houston, Texas 77001

Abstract

Methods for direct and indirect measurements of biofilm development (fouling) are presented. Laboratory systems were developed to determine rate and extent of fouling as a function of wall shear stress, water quality, and bulk temperature. Experimental systems were also developed to evaluate the effects of oxidizing biocides and to compare their relative efficiency.

Fouling, the undesirable deposition of materials on surfaces, is the major cause of energy losses in fluid transport and heat exchange systems. The general term fouling can reflect any or all combinations of the following four processes:

1. Precipitation or crystallization (scaling) - primarily due to precipitation of calcium salts on heated surfaces.
2. Suspended solids - due to sedimentation and adsorption of solid particles on surfaces.
3. Corrosion - production of thermally insulating metal oxide scale from corrosion processes.
4. Biological (or organic) fouling - development of a microbial film possibly followed by a succession of higher life forms.

This paper concerns biological fouling--experimental methods for observing its development, effects, and destruction.

Microbial fouling is a major cause of energy losses in power plant condensor tubes and in long pipelines supplying cooling water to power plants. Thin, viscoelastic biofilms develop on the conduit walls causing unexpectedly large increases in fluid frictional resistance. Characklis (1,2) and Norman(3) have reviewed the literature concerning the growth of biofilm and its effects on frictional resistance.

Biofilms also develop in heat exchange tubes, insulating them and causing reduced efficiency. Steam driven power plants, consumers of 80% of all industrial cooling water in the U.S., encounter significant problems. Reduced efficiency, caused by fouling on condensor surfaces, costs the power industry approximately \$400 million a year for extra fuel which is equivalent to 25 million barrels of oil (4). The fouling is primarily due to microbial growths and their extracellular polymers which accelerate adsorption of fine suspended particles to the heated surfaces.

The films also accelerate corrosion processes in the metal tubes and influence deterioration in wooden cooling towers. Microbial fouling is one of the major barriers to economic utilization of ocean thermal energy conversion and membrane desalina-

tion processes.

Control of biofouling is frequently accomplished by adding chlorine or other oxidants. Application frequency and dose are determined arbitrarily because methods for determining the effectiveness of the chemical additive are unavailable. Economic considerations, energy conservation demands and increasingly stringent regulations on potentially toxic residuals (and their reaction products) require a systematic understanding of factors influencing microbial fouling and its control.

This paper describes several experimental systems and methods developed for observing biofilm development and destruction in the laboratory. Preliminary results using several of these methods are presented along with a phenomenological description of the biofouling process based on our experimental observations.

### Experimental Systems

#### Apparatus

##### Rationale for Design

The objective of this research program is to study the development, effects, and destruction of biofouling films. Environmental factors that can influence these processes must be controlled or be determined easily.

The reaction processes involved are similar to solid-catalyzed reactions and any type of reactor with known contacting pattern may be used to explore the kinetics. In one of our experimental systems, a tubular reactor was used because of its geometric similarity to condenser or heat exchange tubes. A mixed reactor system (i.e., reactor contents spatially uniform) was accomplished by providing a recycle loop and operating at a high recycle ratio (Fig. 1).

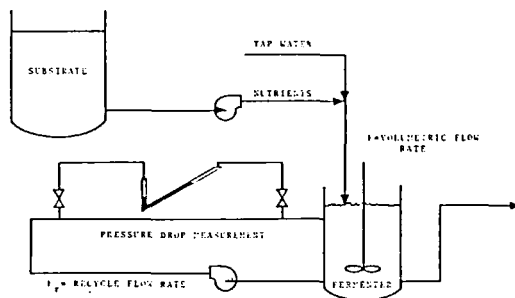


FIG. 1

Schematic diagram of tubular fouling reactor system

A high recycle ratio provides a way of approximating completely mixed conditions with what is essentially a plug flow device. The fouling indicator (Fig. 1) is a manometer which monitors changes in frictional resistance due to biofilm development along a length of the recycle loop. Alternatively, the indicator would be a thermistor system for detecting changes in heat transfer due to film development. Advantages of the system are as follows:

1. At high recycle rates,  $F_r \gg F$ , the reactor contents, (including the internal recycle) are completely mixed. Mathematical description and sampling are simplified since there are no concentration gradients.
2. Biofilms in the recycle section are uniform.
3. Temperature and pH control are simplified and dissolved

- oxygen monitoring can be effectively accomplished in the reactor.
4. Wall shear stress is independent of hydraulic retention time.
  5. Short hydraulic retention times (15 minutes or less) eliminate biomass production in the bulk fluid. Consequently, microbial activity is limited to the reactor surfaces.

The annular fouling reactor (AFR) consists of two concentric cylinders with the inner cylinder rotating (Figures 2 and 3).

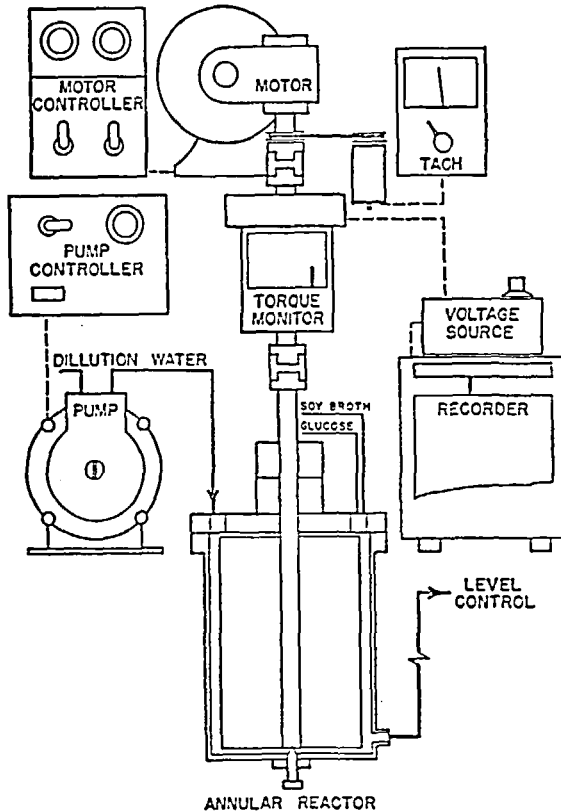


FIG. II

Experimental system for evaluating effect of velocity, water quality, and bulk temperature on biofouling rate (AFR). Also used for determining kinetics of fouling control via chemical treatment (e.g. chlorine, ozone, etc.).

Shear stress (speed of rotation) is independent of hydraulic retention time. The reactor is completely mixed by virtue of the pumping action of four draft tubes and an impeller situated at the bottom of the inner cylinder (5). Therefore, a recycle loop is not necessary. Fouling is indicated by a change in torque monitored by a torque transducer mounted on the drive shaft of the inner cylinder.

#### Biofouling Measurement Techniques

##### Film Thickness Measurement

##### Film Volume

Small tubular test sections (5 cm long) are inserted as an integral part of the tubular reactor (Fig.4).

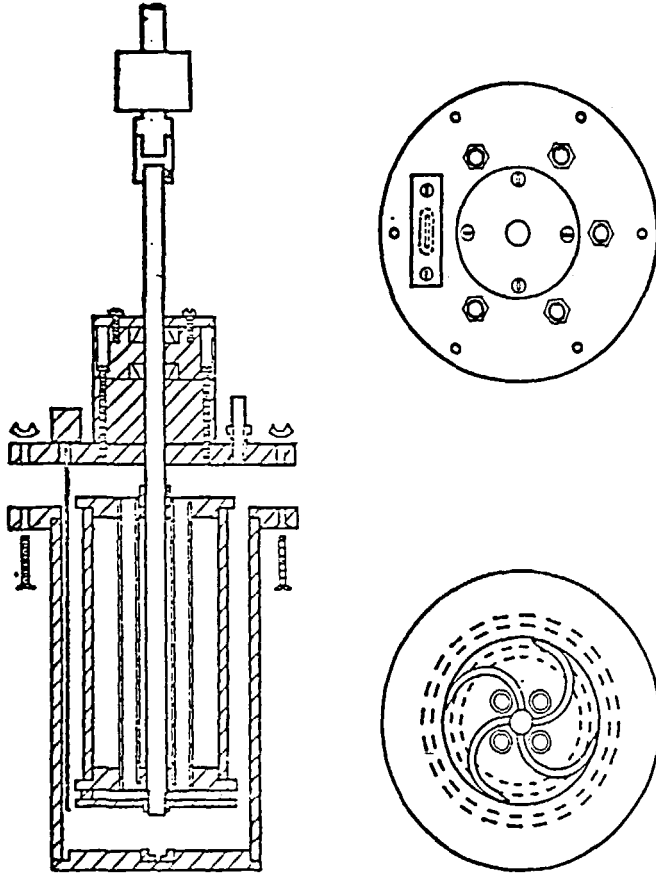


FIG. III  
Annular fouling reactor (AFR) apparatus.

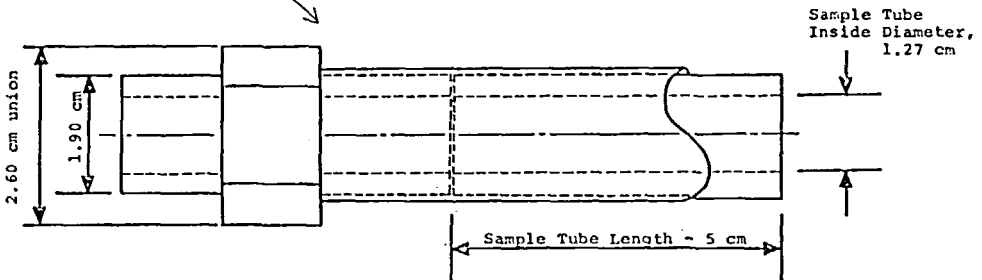
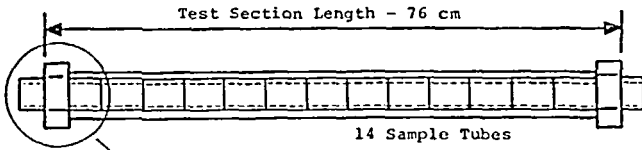


FIG. IV  
Test section and enclosed sample tubes for  
biofilm thickness and mass measurements.

At designated intervals, a tube is removed from the TFR and the volumetric displacement of the biofilm is determined using the apparatus pictured in Figure 5.

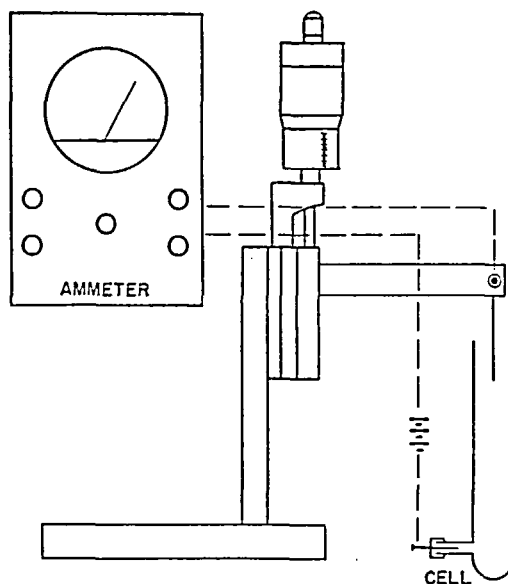


FIG. V

#### Volumetric displacement method for biofilm thickness measurement

The displacement cell is filled with a water-surfactant solution. Initial liquid level (i.e., without the test section immersed) is measured by lowering the conductive probe, by means of a micro-manipulator, until contact is made with the water surface, indicated by deflection of the ammeter. The ammeter is in series with the cell and a 1.5v power source. A 5x1.27 cm (ID) fouled test section is now immersed in the cell and the new liquid level (and hence displacement) due to the fouled test section is determined. The test section is then cleaned, dried, and immersed in the cell. The difference between the displacements of the fouled and clean test section is the film volume. Wet thickness is determined by dividing film volume by the surface area of the test section.

This method was calibrated by measuring displacement of copper wire segments of known mass, and therefore, known volume. Precision is  $\pm 9\mu\text{m}$ . Average inside surface area of the test sections is  $20.0\text{ cm}^2$  with a range of 1.2%.

#### Optical Microscope

This technique was adapted from that of Sanders (6) and requires film growth on a transparent surface. In this case, microbial film develops on a thin acrylic plastic slide which forms an integral part of the AFR reactor wall. The slide is withdrawn from the reactor and placed on a microscope stage. The 10x objective (total magnification = 100x) is lowered until the film surface is in focus and the fine adjustment dial setting is recorded. The objective is then lowered further until the inert plastic growth surface is in focus (Figure 6). The difference in fine adjustment settings is compared with a calibration curve and the thickness obtained.

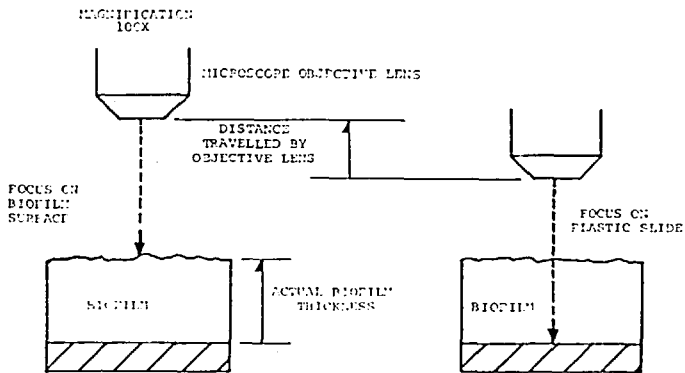


FIG. VI  
Schematic representation of biofilm thickness measurement using an optical microscope

#### Areal Mass Density Measurement

Small test sections (5.0 cm long) are an integral part of the tubular reactor wall. At regular intervals, a test section is removed, dried, and weighed. The tube is then cleaned, dried, and weighed. The tube is then cleaned, dried, and weighed again. The difference is the dry film weight. The length and diameter of the tubes are known so an areal mass density can be calculated. If thickness or volume has also been measured, a wet mass density is obtained.

#### The Frictional Resistance

The development of biofilm on surfaces increases fluid frictional resistance and therefore, energy consumption. Consequently, friction factor ( $f$ ) increase is a good indicator of microbial fouling and biofilm development. In the TFR, friction factor is calculated by the following equation:

$$f = \frac{d}{2L} \frac{\Delta p}{\rho v_m^2}$$

where  $d$  = tube diameter (L)  
 $L$  = tube length (L)  
 $\rho$  = fluid density (M/L<sup>3</sup>)  
 $v_m$  = mean fluid velocity (M/L<sup>3</sup>)  
 $\Delta p$  = pressure drop across length  $L$  (M/L-t<sup>2</sup>)

In the AFR, friction factor is defined as follows:

$$f_a = \frac{T_g}{3 \rho \pi R_i (R_i + R_o) \Omega H}$$

where  $R_i$  = radius of the inner cylinder (L)  
 $R_o$  = radius of the outer cylinder (L)  
 $\Omega$  = rotational velocity (t<sup>-1</sup>)  
 $H$  = height of the cylinders (L)  
 $T_g$  = torque (ML<sup>2</sup>/t<sup>2</sup>)

Torque is measured by a torque transducer mounted to the shaft which drives the inner cylinder. The torque is monitored in the range of 0 - 3.50 N-cm.

## Results and Discussion

### Development of Biofilms

The process of biofilm development on a glass surface due to consumption of a soluble nutrient is adequately described by a sigmoidal-shaped curve which is divided into three regions for convenience of analysis: (1) induction, (2) growth, and (3) plateau. This curve (Figure 7) describes the progression of frictional resistance and heat transfer resistance also. It is assumed that the only suspended solids present are those produced by microbial activity (i.e., volatile solids).

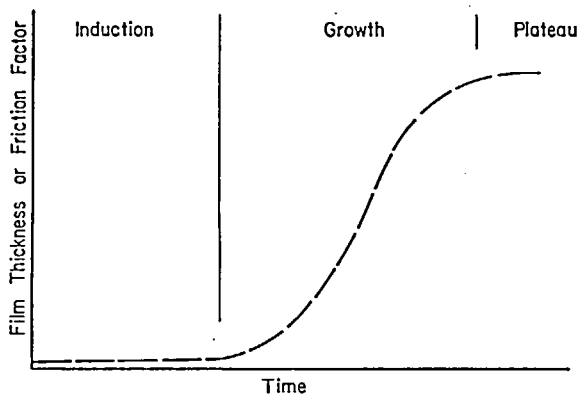


FIG. VII  
Progression of a typical biofouling experiment

### Induction Phase

Previous researchers have indicated that the length of the "induction" period is a function of the attachment surface roughness and composition (1). Quantitative observations of these effects were beyond the scope of this project. It has been noted, however, that the length of the induction period increases with decreasing nutrient loading rates. The accelerated surface activity at high nutrient loading rates could affect the chemical conditioning of the surface and/or, because of increased number of microbial particles (individual cells or flocs) resulting from high nutrient loading rate, the flux of particles to the attachment surface is enhanced. Organic compounds with high surface activity would be expected to adsorb rather quickly (7). The influence of the initial adsorbed films can differentially immobilize boundary layers of liquid approaching 100  $\mu\text{m}$  even on clear surfaces. The influence of such a film would be to decrease convective heat transfer in the initial stages of exposure, an observation made during some of our experiments. The particle properties indicate that their transport to the attachment surface is by inertial deposition and that transport rate increases with increasing particle concentration. Particle attachment, however, will be a function of the characteristics of the particle surface and the attachment surface.

### Growth Phase

Biofilm Development. The logarithmic rate of development (based on biofilm thickness) in the growth phase ( $R^*_{TH}$ ) can be dependent on nutrient loading rate ( $n_g$ ), wall shear stress ( $\tau_w$ ), wall surface temperature ( $T_w$ ), and bulk temperature ( $T_b$ ). The following have been observed in this study (see also Figure 8a):



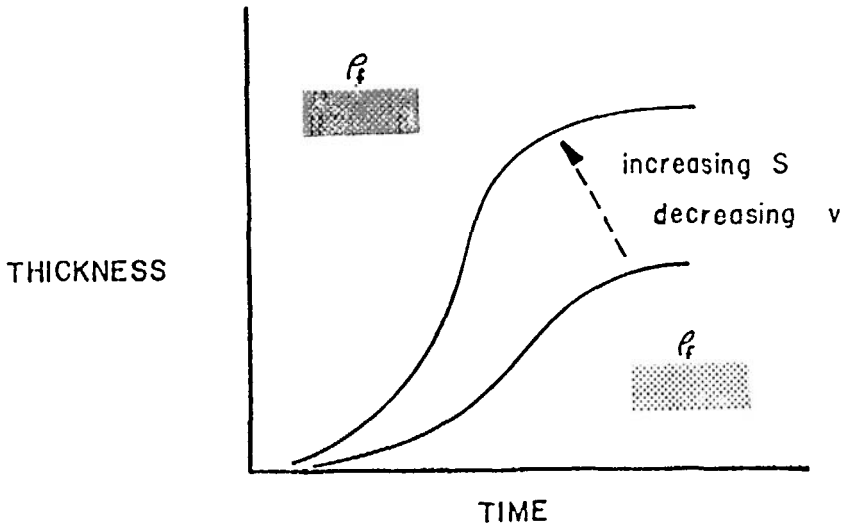


FIG. VIIIa  
Change in biofilm thickness with time during an experiment

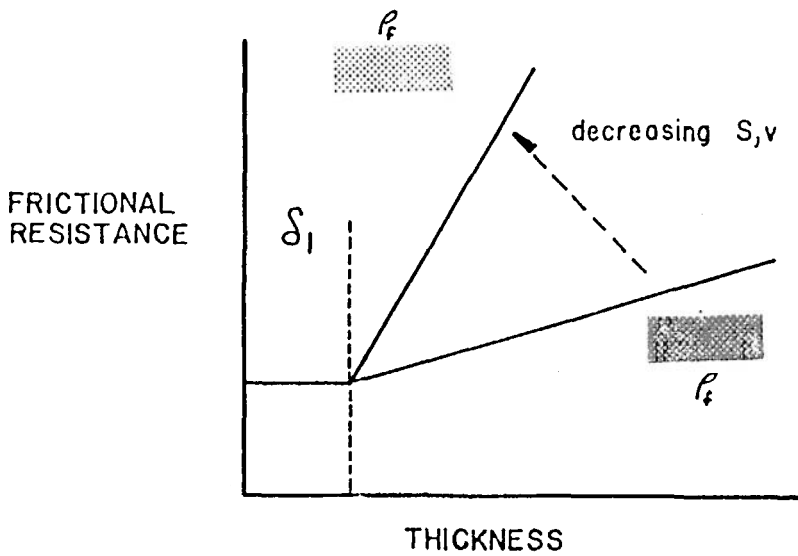


FIG. VIIIb  
Change in frictional resistance related to  
change in biofilm thickness

1.  $R_{th}^*$  increases with increasing  $n_g$  up to some saturating flux. Nutrient removal rate also increases with increasing  $n_g$  up to some saturation value.
2. Increasing  $T_w$  beyond 35°C decreases  $R_{th}^*$ .
3. No significant effect on  $R_{th}^*$  was observed due to change in  $T_b$  (between 30-40°C). However, this result may be due to a suspected optimum temperature of 35°C for  $R_{th}^*$  which made  $R_{th}^*$  relatively insensitive in the temperature range studied. An increase was observed in the logarithmic rate of attached biomass increase of 2.5x when temperature increased from 21 to 31°C during a field study at a power plant.
4. Increasing  $\tau_w$  and  $n_g$  increases biofilm density.

### Plateau Phase

The plateau phase has been characterized by the maximum biofilm thickness ( $Th_{max}$ ).  $Th_{max}$  is strongly dependent on shear stress and less dependent on glucose loading rate in low shear stress ( $\tau_w < 3.0 \text{ N/m}^2$ ) experiments.  $Th_{max}$  is strongly dependent on glucose loading rate and less dependent on shear stress when  $\tau_w > 3.0 \text{ N/m}^2$ . There is some indication from AFR experiments that  $Th_{max}$  was affected by bulk temperature.

The plateau is not necessarily a stable phase. Changes in the biofilm caused by sloughing or changes in morphology (e.g., predominance of filamentous organisms) cause oscillations in biofilm thickness at plateau.

### Frictional Resistance

Growth of the biofilm causes an increase in hydraulic roughness, and therefore, an increase in pressure drop. The "roughness" effect is partially due to the filamentous and rippled nature of the film. The microbial growth begins as isolated colonies which grow by the combined processes of replication and adsorption. The colonies are similar to those observed on agar plates except for the distortion in shape caused by the shear stress. In addition to forming a rippled surface, the biofilm is viscoelastic. This has been determined by *in situ* measurements conducted with a rheogoniometer and results indicate a lightly cross-linked gel with a significant elastic modulus and a very high viscous modulus. The large viscous modulus is the other contributing factor, in addition to the rippled surface, to the excessive energy losses observed in fouled conduits.

A further comment regarding hydraulic roughness is of interest. For turbulent flow through a conduit, a thin laminar (or viscous) boundary layer exists adjacent to the wall. If the roughness elements of the wall lie within this layer, there is no effect on flow properties and the pipe appears hydraulically "smooth". However, if the roughness elements protrude well into the faster turbulent region, they cause drag which reduces local velocities and causes energy losses characteristic of rough surfaces. The thickness of the boundary layer increases with decreasing velocity. Accordingly, the data suggest that the biofilm development has no significant effect on frictional resistance until biofilm thickness reaches some critical value ( $Th_{crit}$ ), at which time, significant changes in frictional resistance occur (Fig. 8b).  $Th_{crit}$  depends on the thickness of the laminary sublayer (directly related to  $\tau_w$ ) and on the film properties which are related to  $\tau_w$  and  $n_g$ .

### Heat transfer Resistance

Biofilm development and resulting increased frictional resistance have been discussed. Changes in heat transfer resistance arise from the combined effects of increased biofilm thickness (conductive heat transfer) and increased frictional resistance (convective heat transfer). Changes in heat transfer resistance due to biofouling film development were observed in a tubular reactor system. Initially, heat transfer decreases for a short period, as expected, due to the insulating effect of the biofilm against conductive heat transfer. Further biofilm development increases hydraulic roughness (as indicated by increasing friction factor) causing higher rates of convective heat transfer. Consequently the rate of increase in heat transfer resistance is not simply related to changes in conductive heat transfer arising from biofilm development (Fig. 9).

### Biofilm Thermal Conductivity

Results indicate that biofilm thermal conductivity is essentially the same as water. This is not a surprising result since biofilm is 90-98% water. It is important to remember that there were no inert suspended solids in the feed to the experimental systems. If particulates with low thermal conductivity become entrapped in highly adsorbent biofilm, the conductive heat transfer resistance will increase at a more rapid rate because of the lower "effective" thermal conductivity of the biofilm.

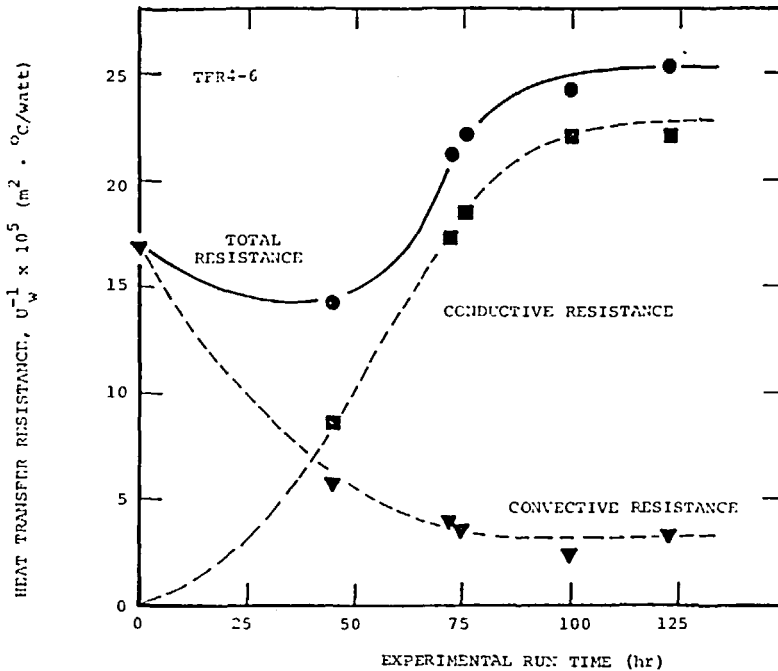


FIG. IX

Change in heat transfer resistance due to biofilm development during an experiment

### Heat Transfer Resistance and Biofilm Development

The effect of glucose loading rate and shear stress at the wall on heat transfer resistance can be calculated from their force on biofilm development rate and the following relationship:

$$\frac{1}{U_w} = \left[ \frac{1}{h} + \frac{r_1 \ln(r_1/r_2)}{k_{Th}} \right]^{-1}$$

$k_{Th}$  is known and  $h$  is a function of Reynolds number, friction factor, and the properties of water. Friction factor increase is related to biofilm development rate as noted above. Our results suggest that we can predict biofilm development rate and its effect on frictional resistance. Therefore, the effect of biofilm development on overall heat transfer resistance can also be calculated from a knowledge of biofilm development rate.

#### Control of Biofouling with Strong Oxidizers

Chlorination has been the predominant means of controlling biofouling. Recently, concern over toxicity of chlorine residuals in natural waters has led to further inquiries into the biofouling control process. Characklis and Dydek(8) showed that chlorine can disrupt microbial film, presumably through hydrolysis of the extracellular polymers which lend structural strength to the deposit. Combined with fluid shear stress, the chemical action results in detachment and partial solubilization of the biofilm (Figure 10). Mercuric chloride inhibited microbial activity (as measured by nutrient and oxygen uptake) but caused no physical changes in the biofilm.

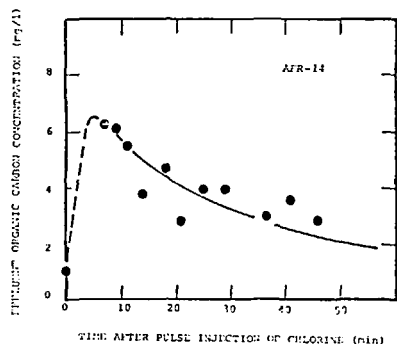


FIG. X

Increase in effluent organic carbon from the AFR following a pulse injection of chlorine.

The increased effluent solids are a result of biofilm hydrolysis

A description of the oxidant-biofilm interaction follows. The first step is transport of the oxidant from the bulk fluid to the biofilm interface. In slow moving fluids, this could be the rate limiting step. The second step is diffusion of the oxidant in the biofilm. Based on our preliminary results, we believe diffusion of the oxidant in the biofilm is the rate limiting step in oxidant consumption (for mean fluid velocities greater than 100cm/sec). Finally, a portion of the weakened biofilm is torn off by fluid shear stress.

Norman et al., (9) describe the effect of chlorination on established biofilms. Figure 11 indicates the effect of chlorine addition on effluent suspended solids, film thickness and pressure drop in the TFR during a typical experiment. Chlorine input was constant for a 30 minute period. The film was partially removed by the chlorine treatment causing an increase in effluent suspended solids (also seen in Fig. 10 for an AFR experiment). Film thick-

ness decreased from 150 to 50  $\mu\text{m}$  and pressure drop was reduced to essentially "clean" conditions.

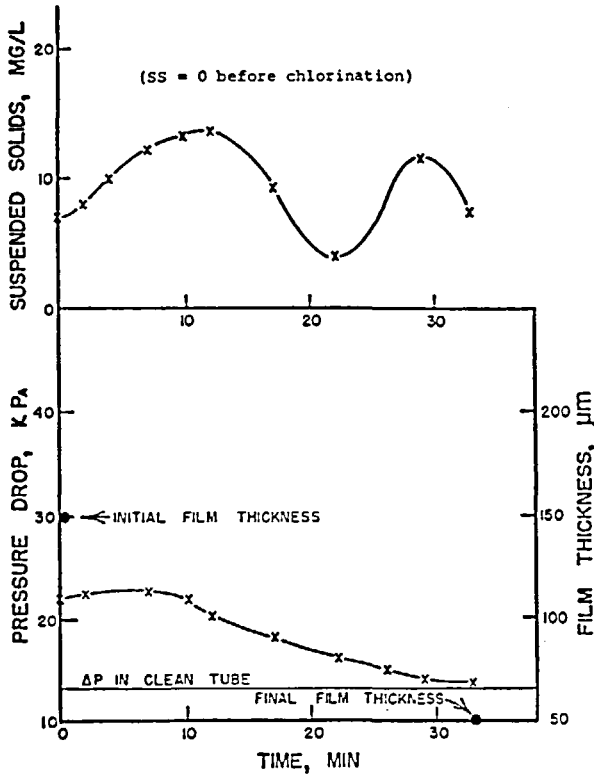


FIG. XI

Pressure drop, thickness, and suspended solids concentration during shock chlorination at 4.1 mg/l. Flow rate = 11.4 l/min.

The effect of dosing level and dosing concentrations is indicated by Fig. 12.

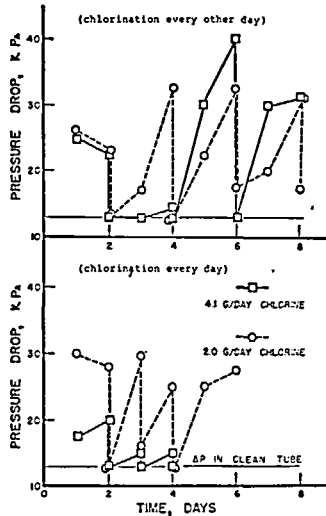


FIG. XII

Shock chlorination effect on frictional resistance

In these experiments, either 2 or 4 grams of chlorine was added over a thirty minute period either every day or every other day. The top graph indicates that a dose of 2 or 4 grams applied every other day is insufficient to control biofouling. In fact, regrowth subsequent to chlorine addition was extremely rapid. The bottom graph indicates that a dose of 2 grams every day was not satisfactory for control. The addition of 4 grams per day, however, was sufficient for maintaining "clean" conditions. Thus, the results suggest that a stoichiometry exists for the chlorination of biofilms, and if the reaction is not carried to completion, the remaining biofilm will catalyze the redevelopment of the film.

Figure 13 indicates the effect of dosing concentration when chlorine is added continuously over a period of two days at a rate of 2 to 4 grams per day. Note the difference in time for regrowth of the biofilm when chlorine addition ceases.

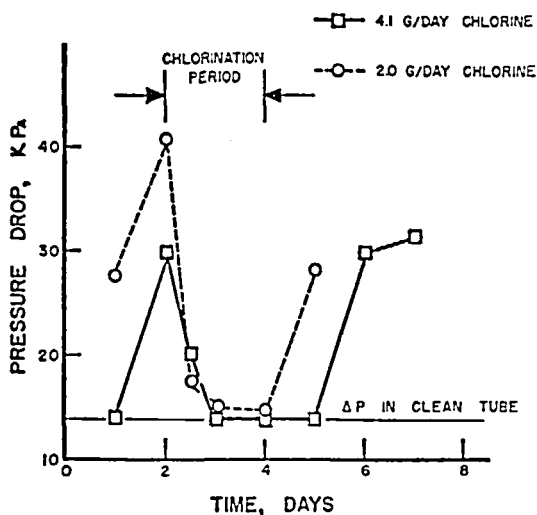


FIG. XIII  
Effect of continuous chlorination on frictional resistance at flow rate = 11.4 l/min.

The AFR proved very useful as a device for testing the relative effectiveness of various chemical oxidants in a given environment. Stoichiometry and kinetics of biofilm destruction can be determined under controlled conditions in this continuous-flow, completely mixed reactor. Figure 14 compares the relative effectiveness of chlorine and hydrogen peroxide in reducing frictional resistance due to biofouling.

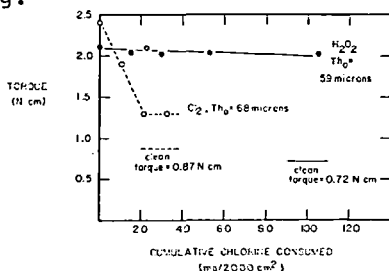


FIG. XIV  
The effect of chlorine and hydrogen peroxide on frictional resistance due to biofouling. Tests conducted in the AFR.

The data indicate a significantly greater decrease in frictional resistance per unit oxidant consumed in the chlorine experiment. Obviously, factors such as oxidant feed concentration, bulk, and surface temperature, fluid shear stress, and pH may affect oxidant effectiveness. Hopefully, future experimentation will provide insight into the effect of these other variables.

#### Summary

Experimental systems and methods have been developed and tested for quantitatively determining biofilm development and its effects on frictional resistance and heat transfer resistance. The same systems can be effectively used to determine the relative effectiveness of chemical control additives.

Continuing research is being directed towards achieving better utilization of the strong oxidants added for biofouling control. Some other classes of compounds used for scale prevention and corrosion control are also being tested.

#### Acknowledgements

The author gratefully acknowledges the following: the National Science Foundation (Grant No. ENG 77-26934) and the Electric Power Research Institute (RP 902-1) for partial financial support; and Linda Graetz for manuscript preparation.

#### References

1. W.G. CHARACKLIS, Attached microbial growths. I. Water Res. 7, 1113-1128 (1973).
2. W.G. CHARACKLIS, Attached microbial growths. II. Frictional resistance due to microbial slimes. Water Res. 7, 1249-1259 (1973).
3. G. NORRMAN, Control of microbial fouling in circular tubes with chlorine, M.S. Thesis, Rice University (1976).
4. R.B. RITTER AND J.W. SUITOR, Fouling research on copper and its alloys -- seawater studies. Progress Report to Intern. Copper Research Assoc., Inc., Heat Transfer Research, Inc., Alhambra, California (1976).
5. B.H. KORNEGAY AND J.F. ANDREWS. Kinetics of fixed film biological reactors, (1968).
6. W.M. SANDERS. The relationship between the oxygen utilization of heterotrophic slime organisms and the wetted perimeter. Ph.D Thesis, Johns Hopkins University (1964).
7. G.I. LOEB AND P.A. NEIHOF, Marine conditioning films. Appl. Chemistry at protein interfaces (R.E. Baker, ed.) Am. Chem. Soc. 319-335 (1975).
8. W.G. CHARACKLIS AND S.T. DYDEK, The influence of carbon to nitrogen ratio on the chlorination of microbial aggregates, Water Res., 10, 515-522 (1976).
9. G. NORRMAN, W.G. CHARACKLIS, AND J.D. BRYERS, Control of microbial fouling in circular tubes with chlorine, Dev. Ind. Microbiol. 18, 581-590 (1977).

#### Key Words

Biofilm, Turbulent flow

#### Auszug

Methoden zur direkten und indirekten Messung der Bildung von Bioschichten (Verunreinigung) werden vorgelegt. Laborverfahren wurden entwickelt, um den Grad und das Ausmass der Verunreinigung als eine Funktion der Wandscherkraft, der

Wasserqualität und der Temperatur zu bestimmen. Versuchsverfahren wurden auch entwickelt, um die Wirkung der zur Oxydierung beitragenden Mitteln festzustellen und ihre relative Leistungsfähigkeit zu vergleichen.

Abrége

Dans cette étude, on présente des méthodes directes et indirectes de mesurer la croissance biologique.